

# Real Gas Effect on Ignition Characteristics in Ideal and Non-ideal Reactors

Zifeng Weng, Zongtai Li, Rémy Mével  
Center for Combustion Energy, School of Vehicle and Mobility,  
Safety and Energy State Key Laboratory for Automotive, Tsinghua University  
Beijing, China

## 1 Introduction

The development of reaction model relies on accurate measurements in well-controlled reactors. Shock tube (ST) creates nearly homogeneous and constant volume (CV) or constant pressure (CP) system and has been widely used to study high-temperature chemical kinetics [1]. Rapid compression machine (RCM) also creates nearly homogeneous and CV conditions, but is mainly employed within the low-to intermediate-temperature ranges [2]. The simulation of ST and RCM experiments usually relies on CV or CP reactor, which, however, are too ideal. Non-ideal effects in ST and RCM were found to significantly modify the chemical dynamics [3, 4] and uncertainty [5] of ignition delay-time (IDT). In ST, linear pressure rise is typically induced by finite diaphragm opening, shock wave attenuation, or boundary layer growth [6]. In RCM, heat loss causes the expansion of the adiabatic core which results in a time-dependent pressure drop [2, 7]. To account for these effects, variable-volume reactors, such as CHEMSHOCK [3] and VTIM [4], have been developed. The CV simulation was corrected with measured pressure traces and adiabatic or polytropic process. Zander et al. used only the slope of the linear pressure variation, instead of a complete pressure trace [8]. Aside from the non-ideal effects, the real gas effect, not considered in many works, might also result in inaccurate simulation results. RCM typically covers the ranges 600-1200 K and 0.5-8 MPa [2], while ST operates from 600 to 3000 K and, from sub-atmospheric pressure to about 100 MPa [1]. While the molecular attraction effect might be minor at high temperature [9], the finite volume effect should be taken into account at elevated pressure. Tang and Brezinsky performed a CV modeling using Peng-Robinson equation of state (EoS), real gas thermodynamics and kinetic law [10]. The real gas effect was found to promote the reaction slightly. Kogekar et al. studied the IDT of n-dodecane/O<sub>2</sub>/N<sub>2</sub> mixtures [11]. The IDT was found to be considerably affected by real gas effect, especially within the negative-temperature-coefficient region. We seek at studying both the non-ideal facility effects and the real gas effect on the ignition characteristics of chemical reactors. In section 2, we establish the dimensionless equations of ideal and non-ideal reactors considering the Noble-Abel (NA) EoS. Parameters were defined to characterize the physical properties of non-ideal reactors. The non-ideal effects and real gas effect on IDT are discussed in section 3.

## 2 Methods

The NA EoS  $P(v - \tilde{b}) = \tilde{R}T$  was adopted to account for the real gas effect. The specific covolume parameter  $\tilde{b}$  represents the finite molecular volume. The molecular interaction was neglected since it is

minor at high temperature [9].  $\tilde{b}$  was related to the critical temperature ( $T_c$ ) and critical pressure ( $P_c$ ) for a given species, i.e.  $\tilde{b} = \tilde{R}T_c/8P_c$ . In gaseous mixture,  $\tilde{b} = \sum_i y_i \tilde{b}_i$ . was used as the mixing rule to calculate  $\tilde{b}$ . The combustion reaction was simplified as an irreversible, first-order, one-step reaction between the reactant  $A$  and the product  $B$ . The reaction progress variable ( $\lambda$ ) follows the Arrhenius law

$$\frac{d\lambda}{dt} = k(1-\lambda)\phi_A \exp\left(-\frac{E_a}{RT}\right), \quad (1)$$

where  $k$  is the rate constant and  $\phi_A$  is the fugacity coefficient of species  $A$ . The fugacity coefficient was used to correct the reaction rate when the state departs from perfect gas (PG) assumption [10]

$$\phi_i = \exp\left(\frac{W_i}{W} \frac{\tilde{b}_i}{v - \tilde{b}}\right). \quad (2)$$

We assumed  $A$  and  $B$  have the same molecule weight ( $W$ ), covolume parameter, heat capacity at constant volume ( $c_v$ ) and pressure ( $c_p$ ). For NA gas, heat capacity and internal energy are the same as for PG. However, enthalpy depends on both temperature and pressure, i.e.  $h = c_p T + \tilde{b}P$ .

The zero-dimensional reactors are derived from the first law of thermodynamics, which reads

$$\frac{de}{dt} = \frac{d\lambda}{dt} Q - P \frac{dv}{dt}, \quad (3)$$

where  $e$  is the internal energy and  $Q$  is the heat release. In order to set up general reactor models, the equation is non-dimensionalized with the following relationships

$$\tilde{T} = \frac{T}{T_1}, \tilde{P} = \frac{P}{P_1}, \tilde{t} = \frac{t}{\tau_v^\circ}, q = \frac{Q}{c_v T_1}, \tilde{v} = \frac{P_1 v}{\tilde{R} T_1}, \beta = \frac{P_1 \tilde{b}}{\tilde{R} T_1}. \quad (4)$$

$T_1$  and  $P_1$  are temperature and pressure at initial state.  $\tau_v^\circ$ , given in Eq. (5), is the asymptotic IDT for PG in CV reactor.  $\theta$  is the reduced activation energy defined as  $E_a/RT_1$ .

$$\tau_v^\circ = \frac{1}{k} \frac{c_v T_1}{Q \theta} \exp(\theta). \quad (5)$$

Using the CV assumption in Eq. (3) and substituting Eq. (4) into Eq. (1) and (3) lead to the CV model

$$\frac{d\tilde{T}}{d\tilde{t}} = \frac{(1-\lambda)}{\theta} \exp\left(\frac{\beta}{\tilde{v}-\beta}\right) \exp\left(\theta - \frac{\theta}{\tilde{T}}\right), \quad (6a)$$

$$\frac{d\lambda}{d\tilde{t}} = \frac{(1-\lambda)}{q\theta} \exp\left(\frac{\beta}{\tilde{v}-\beta}\right) \exp\left(\theta - \frac{\theta}{\tilde{T}}\right). \quad (6b)$$

Similarly, the governing equations for CP reactor can be obtained by replacing  $e$  in Eq. (3) with  $h$  and applying the CP assumption. The derivative of temperature is

$$\frac{d\tilde{T}}{d\tilde{t}} = \frac{(1-\lambda)}{\gamma\theta} \exp\left(\frac{\beta}{\tilde{v}-\beta}\right) \exp\left(\theta - \frac{\theta}{\tilde{T}}\right), \quad (7)$$

where  $\gamma$  is the heat capacity ratio. In non-ideal reactors, pressure and volume vary with time even when no reaction happens. Zander et al. [8] assumed the volume is isentropically changed by non-ideal pressure ( $P_{\text{non}}$ ) variation. For NA gas,  $\tilde{P}(\tilde{v}-\beta)^\gamma$  is constant during an adiabatic process, which leads to

$$\frac{d\tilde{v}}{d\tilde{t}} = -\frac{\tilde{v}-\beta}{\gamma\tilde{P}_{\text{non}}} \frac{d\tilde{P}_{\text{non}}}{d\tilde{t}}, \quad (8)$$

Substituting Eq. (1) and (8) into Eq. (3) leads to

$$\frac{d\tilde{T}}{d\tilde{t}} = \frac{(1-\lambda)}{\theta} \exp\left(\frac{\beta}{\tilde{v}-\beta}\right) \exp\left(\theta - \frac{\theta}{\tilde{T}}\right) - (\gamma-1)\tilde{P}_{\text{non}}\frac{d\tilde{v}}{d\tilde{t}}. \quad (9)$$

In ST, the linear pressure rise is modeled with a constant compression (CC) reactor. The pressure variation is described with a constant compression rate ( $\kappa$ ) given by

$$\frac{d\tilde{P}_{\text{non}}}{d\tilde{t}} = \kappa \text{ or } \tilde{P}_{\text{non}} = \kappa\tilde{t} + 1. \quad (10)$$

Since the time is non-dimensionalized with  $\tau_v^\circ$  and  $\tilde{P}_{\text{non}}(1) = 1 + \kappa$ ,  $\kappa$  approximately represents the percentage of pressure rise during the ignition delay-time. In RCM, the pressure decreases logarithmically as presented in Fig. 1. A logarithmic expansion (LE) reactor is designed, in which the pressure is governed by

$$\frac{d\tilde{P}_{\text{non}}}{d\tilde{t}} = -\frac{n}{m+\tilde{t}} \text{ or } \tilde{P}_{\text{non}} = 1 - n \ln\left(1 + \frac{\tilde{t}}{m}\right) \quad (11)$$

However, the physical meanings of  $n$  and  $m$  are not clear. We further defined the pressure decay rate at  $\tilde{t} = 0$  as  $\kappa_1$  and the percentage of pressure decreasing at  $\tilde{t} = 1$  as  $\kappa_2$ . It is clear that  $\tilde{P}_{\text{non}}$  falls in the range  $(1 - \kappa_1\tilde{t}, 1]$  and  $\kappa_1 \geq \kappa_2$ . As a result,  $\kappa_1$  is not only the maximum decay rate of  $\tilde{P}_{\text{non}}$ , but also the upper bound of pressure decreasing percentage in the ignition delay period.

$$\kappa_1 = -\frac{d\tilde{P}_{\text{non}}(0)}{d\tilde{t}}, \quad \kappa_2 = 1 - \tilde{P}_{\text{non}}(1). \quad (12)$$

In above models,  $\beta$  represents the real gas effect while  $\kappa$ ,  $n$  and  $m$  (or  $\kappa_1$  and  $\kappa_2$ ) reflect the non-ideal facility effects. The range of  $\beta$  is determined by evaluating its order of magnitude for several species, including  $\text{H}_2$ ,  $\text{N}_2$  and  $\text{C}_1$ - $\text{C}_4$  alkanes.  $\beta$  is on the order of  $O(10^{-3})$  at ambient pressure, and increases to order 1 at 100 MPa.  $\kappa$  was obtained based on work of Nativel et al. [12]. They found that  $d\tilde{P}/d\tilde{t}$  was in the range 0-12%  $\text{ms}^{-1}$  for their facilities. To extensively cover this range, we assumed  $\kappa$  is within 0-20%. The parameters  $n$  and  $m$  were obtained by fitting the pressure data measured by Mittal et al. [13, 14] and Sarathy et al. [15], as presented in Fig. 1. We set  $\tau_v^\circ$  to 10 ms to normalize the experimental data shown in Fig. 1. Among all the experimental cases,  $\kappa_1$  is less than 0.5 and  $\kappa_2$  is less than 0.18. Both of them increase with  $\tau_v^\circ$ . In our simulations, we set  $\kappa_1$  to 0-0.5 while the maximum value of  $\kappa_2$  was set to 0.2 to make it consistent with the range of  $\kappa$ . The values of  $n$  and  $m$  can be uniquely determined given a set of  $\kappa_1$  and  $\kappa_2$ .

### 3 Results and Discussion

The pressure and temperature profiles of ideal and non-ideal reactors are shown in Fig. 2. Both PG and NA EoS ( $\beta = 0.1$ ) were applied. The compression rate of CC reactor is 20%. For LE reactor,  $(\kappa_1, \kappa_2) = (0.5, 0.2)$  and the pressure decreases by 20% at  $\tilde{t} = 1$ . Compared to the results calculated with PG EoS, the use of NA EoS increases the reaction rate for all reactors, but the final states are not affected. In CV reactor, all the heat released is used to increase the temperature to the adiabatic flame temperature. The compression in CC reactor provides additional work to promotes the ignition and raises the final pressure and temperature. The compression couples with the real gas effect to further reduce the IDT. In contrast, the expansion in LE reactor slows down the ignition and results in lower final pressure and temperature. It also diminishes the real gas effect. For the specific conditions we used, the ignition in LE reactor happens at a time closed to that of the CP reactor. However, in CP reactor, the

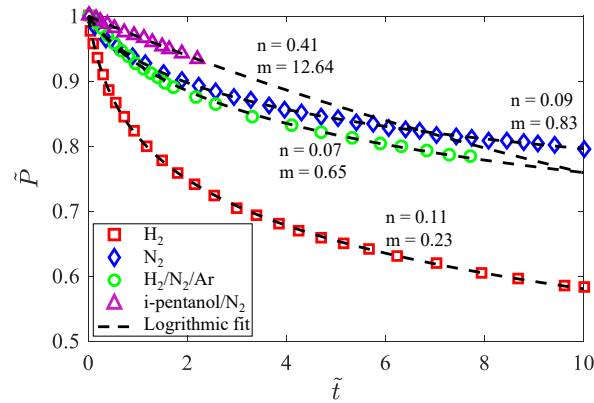


Figure 1: Pressure traces of four inert mixtures measured in RCM. Symbols are experimental data taken from Mittal et al. [13, 14] and Sarathy et al. [15]. Dashed line are fitting results using Eq. (11). The pressure was normalized with its value at the end of compression.  $\tau_v^{\circ}$  was taken as 10 ms.

system expands very rapidly and by a large amount to maintain the pressure at its initial value. For the LE reactor, the expansion rate is much lower and the amount of expansion is more limited as described by the adiabatic core hypothesis [7]. As a result, the final temperature and pressure of CP reactor are much lower than the values of LE reactor.

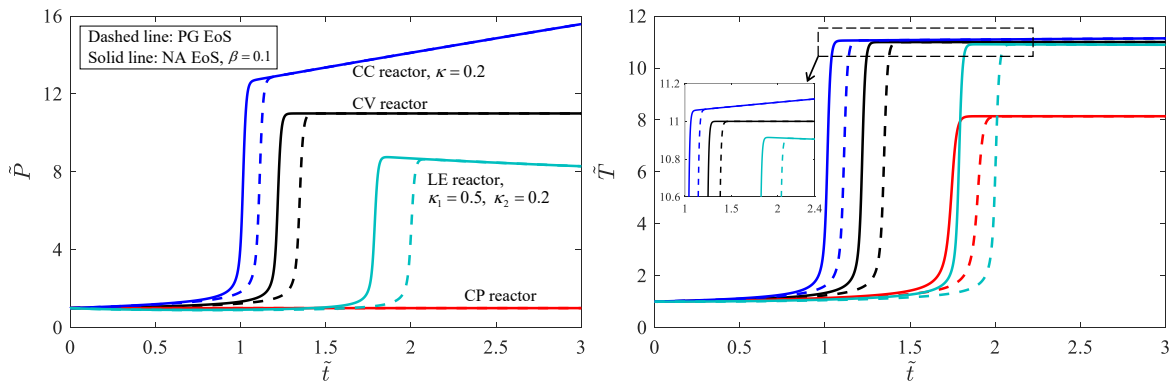


Figure 2: The pressure and temperature profiles of ideal and non-ideal reactors using both ideal EoS (dashed line) and NA EoS (solid line).  $\beta$  is 0.1,  $\gamma$  is 1.4,  $q$  and  $\theta$  are both 10.  $\kappa$  of CC reactor is 0.2 while  $\kappa_1$  and  $\kappa_2$  of LE reactor are 0.5 and 0.2, respectively.

The ignition characteristics of ideal and non-ideal reactors were characterized by their IDT ( $\tilde{t}_{ig}$ ), which was defined as the time to reach maximum temperature gradient. Figure 3(a) presents the IDT of ideal reactors calculated with NA EoS. The results were normalized with the IDT of PG in the same reactors, denoted with superscript  $\circ$ . The IDT of both CV and CP reactors decreases monotonically with  $\beta$ . When  $\beta$  is less than  $10^{-2}$ , the real gas effect is negligible. As  $\beta$  increases to  $10^{-1}$ , the use of NA EoS decreases the IDT by about 10%. When  $\beta$  is in the range of 0.1-1.0, the real gas effect becomes significant as the IDT ratio drops much faster. In addition,  $\beta$  has larger impact on CV reactor compared to the result of CP reactor. It is noted that the IDT ratios were found to be almost the same for different  $\gamma$ . The IDT of CC reactor was presented in Fig. 3(b). The compression rate was 0.01 to 0.2 while  $\gamma$  was 1.2 to 1.4. The results were normalized with the IDT of PG, CV reactor. The effect of  $\beta$  on IDT of CC reactor is similar to the case in ideal reactor. In addition, the compression promotes the ignition and with higher compression rate, the IDT is shorter. The effect of compression is closely related to  $\gamma$ . When  $\gamma$  is 1.4, a 10% compression rate decreases the IDT of PG by 10%. However, for  $\gamma = 1.2$ , about 20% compression

rate is needed to achieve the same result. The effect of  $\gamma$  is also affected by the compression rate. When  $\kappa$  is larger, the IDT is more sensitive to the change of  $\gamma$ . In CC reactor, both the real gas effect and non-ideal effect contribute to speed up the ignition. When  $\beta$  is small, the non-ideal effect is the dominated one. However, when  $\beta$  is larger than 0.1, the real gas effect becomes dominant since all the curves tend to converge as  $\beta$  increases.

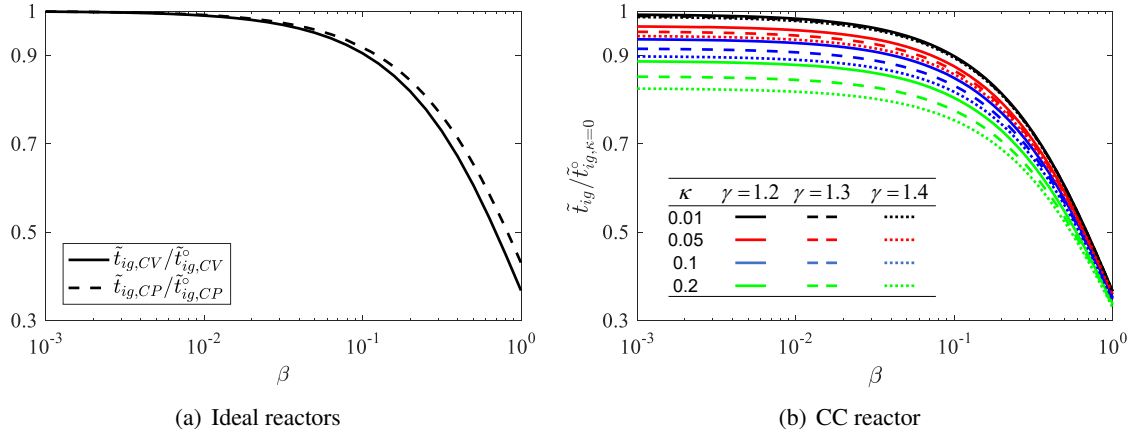


Figure 3: IDT of (a) ideal reactors and (b) CC reactor with different compression rates for  $\beta$  ranging from  $10^{-3}$  to  $10^0$ . The results are normalized with the IDT calculated with PG.  $\theta$  and  $q$  are both 10.  $\gamma$  is 1.4 in (a) and 1.2-1.4 in (b).

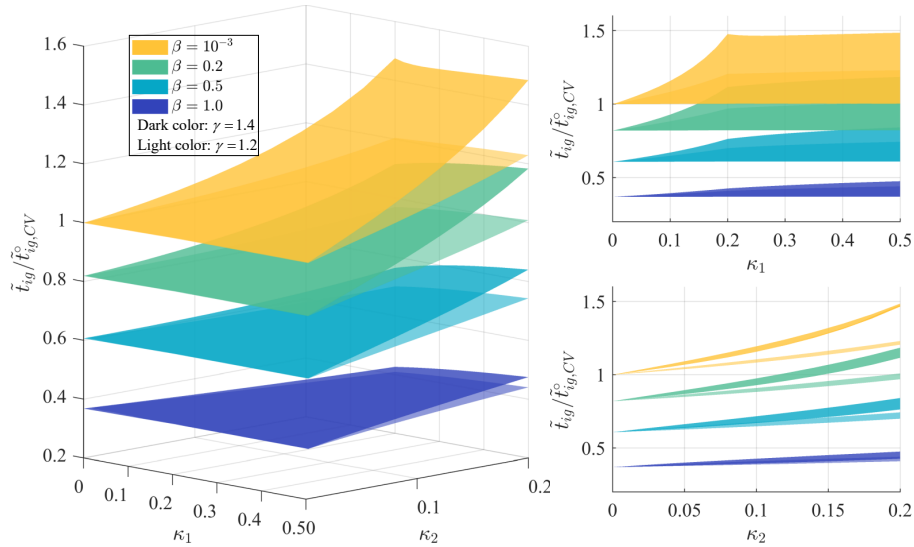


Figure 4: IDT of LE reactor for  $\kappa_1 \in [0, 0.5]$  and  $\kappa_2 \in [0, \max\{\kappa_1, 0.2\}]$ . The left figure is a three-dimensional view while the right figures are projections in two directions. The results were normalized with the IDT of PG, CV model ( $\beta, \kappa_1, \kappa_2 = 0$ ).  $\beta$  falls in  $10^{-3}$ -1.0.  $\gamma$  is 1.2 (light color) and 1.4 (dark color).  $q$  and  $\theta$  are both 10.

Figure 4 presents the IDT of LE reactor for  $\kappa_1 \in [0, 0.5]$  and  $\kappa_2 \in [0, \max\{\kappa_1, 0.2\}]$ .  $\beta$  was  $10^{-3}$ -1.0.  $\gamma$  was 1.2 and 1.4. The results in Fig. 2 and 3 have revealed that the real gas effect tends to speed up the ignition, but the expansion slow down the reaction. These two effects are also affected by the value of  $\gamma$ . These three factors counterbalance each other in the LE reactor simulation. When  $\beta$  is small, the expansion is the dominant effect which increases the IDT. As  $\beta$  increases, the real gas effect gradually diminishes the effect of expansion. Take  $(\beta, \gamma) = (0.2, 1.4)$  as an example, the IDT ratio is smaller than

1 when expansion is slow, but is larger than 1 when expansion becomes strong. With a larger  $\beta$ , the real gas effect dominates. In addition, the decrease of  $\gamma$  attenuates the effect of expansion and thus results in a faster reaction. For clarity, the projection in the  $\tilde{t}/\tilde{t}_{CV-\kappa_1}^\circ$  plane and  $\tilde{t}/\tilde{t}_{CV-\kappa_2}^\circ$  plane are also shown in Fig. 4. As  $\beta$  increases, both the projection area and the slope decreases continuously. In addition, the projection in  $\tilde{t}/\tilde{t}_{CV-\kappa_2}^\circ$  plane converges to a small area, which indicates that the IDT ratio is more sensitive to  $\kappa_2$  than to  $\kappa_1$ . Recalling the physical indication of  $\kappa_1$  and  $\kappa_2$ , it indicates that the IDT ratio is more sensitive to the magnitude of pressure decrease than to the decay rate.

In the discussion of CC and LE reactors, it was found that the non-ideal pressure variation is crucial especially when  $\kappa$ ,  $\kappa_1$  or  $\kappa_2$  are large. The definition and determination of their ranges in section 2 reveal that  $\kappa$ ,  $\kappa_1$  and  $\kappa_2$  tend to increase when the asymptotic IDT ( $\tau_v^\circ$ ) is large. The dimensional  $d\tilde{P}/dt$  is mainly determined by the facility geometry and operation conditions [12]. However, the dimensionless  $d\tilde{P}/d\tilde{t}$  is also affected by the ignition property of the given mixture. The discussion above indicates that at long test time, usually on the order of milliseconds, the non-ideal pressure variation will strongly affect the ignition and thus the experimental or simulation data should be carefully interpreted.

## 4 Conclusion

We studied the real gas effect on the ignition characteristics in ideal and non-ideal reactors with one-step irreversible reaction. The Noble-Abel equation of state describes the finite molecular volume effect, but neglects the molecular attraction. The pressure rise in ST was modeled with a linear function while the pressure decay in RCM was accurately reproduced by a logarithmic function. In all cases, the real gas effect promotes the ignition. The compression couples with the real gas effect to further reduce the ignition delay-time. On the contrary, in LE reactor, the expansion diminishes the real gas effect. The heat capacity ratio becomes important when the non-ideal pressure change is strong. In practice, the non-ideal effect has larger impact on simulation results for longer test time. However, the real gas effect is the dominant factor when the dimensionless covolume parameter reaches 0.1 or above.

## References

- [1] Hanson RK, Davidson DF. (2014). Prog. Energy Combust. Sci. 44:103.
- [2] Goldsborough S, et al. (2017). Prog. Energy Combust. Sci. 63: 1.
- [3] Li H, Owens Z, Davidson D, Hanson R. (2008). Int. J. Chem. Kinet. 40: 189.
- [4] Chaos M, Dryer F. (2010). Int. J. Chem. Kinet. 42: 143.
- [5] Petersen EL, Hanson RK. (2001). Shock Waves. 10:405.
- [6] Hong Z, Pang G, Vasu S, Davidson D, Hanson R. (2009). Shock Waves. 19: 113.
- [7] Sung CJ, Curran HJ. (2014) Prog. Energy Combust. Sci. 44: 1.
- [8] Zander L, Vinkeloe J, Djordjevic N. (2021). Int. J. Chem. Kinet. 53: 611.
- [9] Taileb S, Melguizo-Gavilanes J, Chinnayya A. (2021). Phys. Fluids. 3: 036105
- [10] Tang W, Brezinsky K. (2006). Int. J. Chem. Kinet. 38: 75.
- [11] Kogekar G, et al. (2018). Combust. Flame. 189: 1.
- [12] Nativel D, et al. (2020). Combust. Flame. 217:200.
- [13] Mittal G, Sung CJ. (2007). Combust. Sci. Technol. 179: 497.
- [14] Mittal G, Raju MP, Sung CJ. (2008). Combust. Flame. 155: 417.
- [15] Sarathy SM, et al. (2013). Combust. Flame. 160: 2712.